

# The Effect of Carrier Frequency Offsets on Downlink and Uplink MC-DS-CDMA

Heidi Steendam and Marc Moeneclaey, *Senior Member, IEEE*

**Abstract**—In this paper, we study the sensitivity of uplink and downlink MC-DS-CDMA to carrier frequency offsets, assuming orthogonal spreading sequences. For both uplink and downlink MC-DS-CDMA, we show that the performance rapidly degrades for an increasing ratio of maximum frequency offset to carrier spacing. We point out that the degradation in the uplink is larger than in the downlink because only the former is affected by multiuser interference. For a given (small) ratio of maximum frequency offset to carrier spacing, enlarging the spreading factor in a fully loaded system does not affect the downlink degradation but strongly increases the uplink degradation. Finally, we show that the downlink degradations of MC-DS-CDMA and fully loaded MC-CDMA are the same, provided that for both systems the ratio of frequency offset to carrier spacing is the same.

**Index Terms**—Carrier frequency offset, MC-DS-CDMA, synchronization.

## I. INTRODUCTION

**D**UE TO the enormous growth of wireless services (cellular telephones, wireless local-area networks, etc.) during the last decade, the need for a modulation technique that can reliably transmit high data rates at a high bandwidth efficiency arises. Multicarrier (MC) systems in particular have received considerable attention, as they combine a high bandwidth efficiency with a robustness against multipath distortion [1]–[8]. These MC systems include different combinations of multicarrier modulation and code-division multiple access (CDMA) that have been investigated in the context of high-rate multiuser communication over multipath channels [5]–[8].

A major disadvantage of multicarrier systems is their high sensitivity to frequency offsets between the carrier oscillators at the transmitter and the receiver, especially when the number of carriers is large. The effect of carrier frequency offsets on multicarrier systems has been reported in [9] for orthogonal frequency-division multiplexing (OFDM) and in [10], [11] for MC-CDMA (which combines multicarrier modulation with frequency-domain spreading).

In this contribution, we investigate the effect of carrier frequency offsets on multicarrier direct-sequence CDMA (MC-DS-CDMA), which combines multicarrier modulation with time-domain spreading [5], [7]. In Section II, we describe the uplink and downlink MC-DS-CDMA systems. Analytical

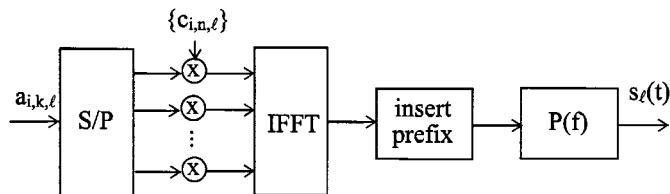


Fig. 1. MC-DS-CDMA transmitter for a single user.

expressions for the system performance in the presence of carrier frequency offset are derived in Section III. In Section IV, we discuss the performance results for downlink and uplink transmission. The MC-DS-CDMA and MC-CDMA performances in the presence of carrier frequency offset are compared in Section V. Conclusions are drawn in Section VI. One of the main conclusions is that MC-DS-CDMA is much more sensitive to frequency offsets in the uplink than in the downlink, especially when the spreading factor is large.

## II. SYSTEM DESCRIPTION

### A. Uplink MC-DS-CDMA

The conceptual block diagram of the transmitter of an MC-DS-CDMA system is shown in Fig. 1 for a single user. In MC-DS-CDMA, the complex data symbols to be transmitted at a rate  $R_s$  are split into  $N_c$  symbol sequences, each having a rate  $R_s/N_c$  and each modulating a different carrier of the multicarrier system. The data symbol  $a_{i,k,\ell}$  denotes the  $i$ th data symbol transmitted by user  $\ell$  on the carrier with index  $k$ , with  $k$  belonging to a set  $I_c$  of  $N_c$  carrier indexes. The symbol  $a_{i,k,\ell}$  is multiplied with a spreading sequence  $\{c_{i,n,\ell}|n = 0, \dots, N_s - 1\}$  with spreading factor  $N_s$ ;  $c_{i,n,\ell}$  denotes the  $n$ th chip of the sequence that spreads the data symbols transmitted by user  $\ell$  during the  $i$ th symbol interval. Note that the spreading sequence does not depend on the carrier index  $k$ : the same spreading sequence is used on all  $N_c$  carriers. It is assumed that  $|c_{i,n,\ell}| = 1$ . The  $N_s$  components of the spread data symbol  $a_{i,k,\ell}$  are denoted  $\{b_{i,k,n,\ell}|n = 0, \dots, N_s - 1\}$ , with

$$b_{i,k,n,\ell} = \frac{a_{i,k,\ell} c_{i,n,\ell}}{\sqrt{N_s}} \quad n = 0, \dots, N_s - 1; k \in I_c. \quad (1)$$

The components  $b_{i,k,n,\ell}$  are serially transmitted on the  $k$ th carrier of an orthogonal multicarrier system, i.e., the data symbols are spread in the time domain (see Fig. 2). The modulation of the spread data symbols on the orthogonal carriers is accomplished by means of an  $N_F$ -point inverse fast Fourier transform (IFFT). To avoid having the multipath channel cause interference between the data symbols at the receiver, each FFT block

Manuscript received February 15, 2001; revised July 6, 2001. This work was supported by the Belgian National Fund for Scientific Research (FWO Flanders). This paper was presented in part at the Vehicular Technology Conference—Spring (VTC'01-Spring), Rhodes Island, Greece, May 6–9, 2001.

The authors are with the Telecommunications and Information Processing (TELIN) Department, Ghent University, Gent B-9000, Belgium (e-mail: Heidi.Steendam@telin.rug.ac.be; Marc.Moeneclaey@telin.rug.ac.be).

Publisher Item Identifier S 0733-8716(01)10299-4.

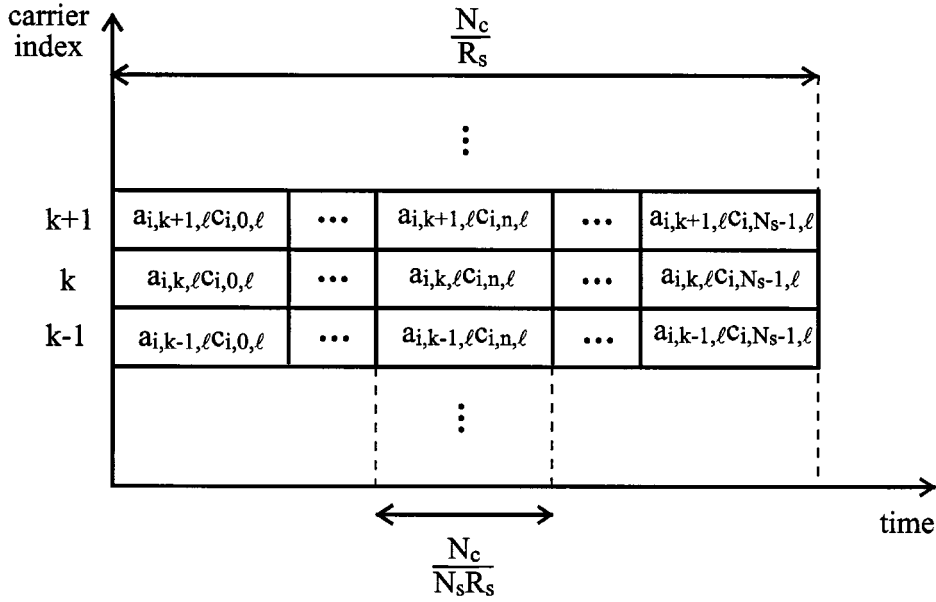


Fig. 2. Illustration of time-domain spreading in MC-DS-CDMA.

at the inverse FFT output is cyclically extended with a prefix of  $N_p$  samples. This results in the sequence of samples  $s_{i,m,n,\ell}$ , with

$$s_{i,m,n,\ell} = \frac{1}{\sqrt{N_F + N_p}} \sum_{k \in I_c} b_{i,k,n,\ell} e^{j2\pi(km/N_F)} \quad (2)$$

$$m = -N_p, \dots, N_F - 1.$$

The transmitter feeds the samples  $s_{i,m,n,\ell}$  at a rate  $1/T = (N_F + N_p)N_s R_s / N_c$  to a square-root raised-cosine filter  $P(f)$  with rolloff  $\alpha$  and unit-energy impulse response  $p(t)$ , yielding the continuous-time transmitted complex baseband signal  $s_\ell(t)$ , given by

$$s_\ell(t) = \sum_{i=-\infty}^{+\infty} \sum_{m=-N_p}^{N_F-1} \sum_{n=0}^{N_s-1} s_{i,m,n,\ell} \cdot p(t - (m + (n + iN_s)(N_F + N_p))T). \quad (3)$$

Because of the normalization factors introduced in (1) and (2), the transmitted energy per symbol on the  $k$ th carrier from user  $\ell$  is given by  $E_{sk,\ell} = E[|a_{i,k,\ell}|^2]$ . It is assumed that carriers inside the rolloff area of the transmit filter are not modulated, i.e., they have zero amplitude. Hence, of the  $N_F$  available carriers, only  $N_c$  carriers are actually used ( $N_c \leq (1 - \alpha)N_F$ ). The carrier index  $k$  corresponds to the carrier frequency  $k/(N_F T)$ . Assuming  $N_c$  to be odd, the set  $I_c$  of carriers actually used is given by  $I_c = \{0, \dots, N_c/2 - 1\} \cup \{N_F - (N_c/2 - 1), \dots, N_F - 1\}$ . The corresponding carrier spacing  $\Delta f$  and system bandwidth  $B$  are given by

$$\Delta f = \frac{1}{N_F T} = \frac{N_s}{N_c} R_s \frac{N_F + N_p}{N_F} \cong \frac{N_s}{N_c} R_s$$

$$B = N_c \Delta f = \frac{N_c}{N_F T} = N_s R_s \frac{N_F + N_p}{N_F} \cong N_s R_s. \quad (4)$$

The above approximations are valid for  $N_p \ll N_F$ .

When several users are active, each user transmits to the basestation a similar signal  $s_\ell(t)$ . To separate the different

user signals at the receiver, each user is assigned a unique spreading sequence  $\{c_{i,n,\ell}\}$ , with  $\ell$  denoting the user index. In this paper, we consider orthogonal sequences, consisting of user-dependent Walsh–Hadamard sequences of length  $N_s$ , multiplied with a complex-valued random scrambling sequence that is common to all  $N_u$  active users. Hence, the maximum number of users that can be accommodated equals  $N_s$ . Without loss of generality, we focus on the detection of the data symbols transmitted by the reference user ( $\ell = 0$ ).

The signal  $s_\ell(t)$  transmitted by user  $\ell$  reaches the basestation through a multipath channel with transfer function  $H_{ch\ell}(f)$  that depends on the user index  $\ell$  [see Fig. 3(a)]. We assume that the timing phase of the transmitter and the time delay introduced by the channel are included in the transfer function  $H_{ch\ell}(f)$ . The output of the channel is affected by a carrier phase error  $\phi_\ell(t) = 2\pi\Delta F_\ell t + \phi_\ell(0)$ , where  $\Delta F_\ell$  denotes a small carrier frequency offset ( $|\Delta F_\ell T| \ll 1$ ). The basestation receives the sum of the resulting user signals and an additive white Gaussian noise (AWGN) process  $w(t)$ . The real and imaginary parts of  $w(t)$  are uncorrelated, and each has a power spectral density of  $N_0/2$ . The contribution from each user is affected by a different carrier frequency offset  $\Delta F_\ell$ , as each user signal is upconverted by a different carrier oscillator.

The resulting signal is applied to the receiver filter, which is matched to the transmit filter, and sampled at a rate  $1/T$  (see Fig. 4). The  $N_F + N_p$  sampling instants and associated samples of the FFT block that correspond to the  $n$ th chip of the  $i$ th symbol on any carrier are denoted  $t_{i,n,m}$  and  $v_{i,n,m}$ , respectively, where

$$t_{i,n,m} = mT + (n + iN_s)(N_F + N_p)T$$

$$m = -N_p, \dots, N_F - 1. \quad (5)$$

From each FFT block of  $N_F + N_p$  samples, the receiver removes the  $N_p$  samples that correspond to the cyclic prefix and keeps the remaining  $N_F$  samples for further processing. These samples are applied to an  $N_F$ -point FFT, followed by one-tap equalizers

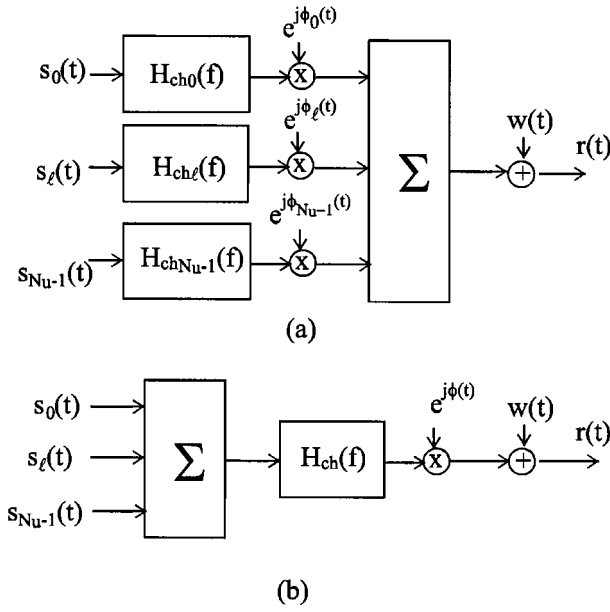


Fig. 3. Channel structure for (a) uplink and (b) downlink.

that scale and rotate the FFT outputs. We denote by  $g_{i,k,n}$  the coefficient of the equalizer, operating on the FFT output with index  $k$  during the  $n$ th FFT block of the  $i$ th symbol interval. The resulting equalizer outputs are multiplied with the corresponding chip of the reference user's spreading sequence and summed over  $N_s$  consecutive values to yield the samples  $z_{i,k}$  at the input of the decision device.

Assuming that the length of the cyclic prefix is longer than the maximum duration of the impulse responses of the composite channels with transfer functions  $H_\ell(f) = |P(f)|^2 H_{ch\ell}(f)$  ( $\ell = 0, \dots, N_u - 1$ ), no interference between successive FFT blocks is introduced, as far as the samples outside the cyclic prefix are concerned (see Fig. 5). In this case, the  $N_F$  samples kept for further processing are given by

$$v_{i,n,m} = \sum_{\ell=0}^{N_u-1} e^{j\phi_\ell(t_{i,n,m})} \sum_{k' \in I_c} \frac{\tilde{a}_{i,k',\ell} c_{i,n,\ell}}{\sqrt{(N_F + N_P)N_s}} \cdot e^{j2\pi(mk'/N_F)} + w_{i,n,m} \quad m = 0, \dots, N_F - 1 \quad (6)$$

where

$$\tilde{a}_{i,k',\ell} = a_{i,k',\ell} H_{k',\ell} \quad (7)$$

and  $H_\ell = H_\ell(\text{mod}(k; N_F)/(N_F T))/T$ , where  $\text{mod}(x; N_F)$  is the modulo- $N_F$  reduction of  $x$ , yielding a result in the interval  $[-N_F/2, N_F/2]$ . The term  $w_{i,n,m}$  denotes the additive noise contribution, with  $E[w_{i,n,m} w_{i,n',m'}^*] = N_0 \delta_{m-m'} \delta_{n-n'}$ . We observe from (6) that the effect of the multipath channel is to multiply the symbol  $a_{i,k',\ell}$  with the factor  $H_{k',\ell}$ , which depends neither on the chip index  $n$  nor on the sample index  $m$ . The carrier frequency offset  $\Delta F_\ell$  is contained in  $\phi_\ell(\cdot)$  and gives rise to a rotation (at a speed of  $2\pi \Delta F_\ell T$  rad/sample) of the contribution from user  $\ell$ .

Denoting by  $V_{i,n,k}$  the  $k$ th output of the FFT processor operating on  $v_{i,n,m}$ , we obtain from (6)

$$\begin{aligned} V_{i,n,k} &= \frac{1}{\sqrt{N_F}} \sum_{m=0}^{N_F-1} v_{i,n,m} e^{-j2\pi(km/N_F)} \\ &= \sqrt{\frac{N_F}{N_F + N_P}} \sum_{\ell=0}^{N_u-1} \frac{\tilde{c}_{i,n,\ell}}{\sqrt{N_s}} \sum_{k' \in I_c} \tilde{a}_{i,k',\ell} M_{k,k',\ell} \\ &\quad + W_{i,n,k} \quad k \in I_c \end{aligned} \quad (8)$$

where

$$\tilde{c}_{i,n,\ell} = c_{i,n,\ell} e^{j\phi_\ell(0)} e^{j2\pi \Delta F_\ell T (n+iN_s)(N_F+N_P)} \quad (9)$$

$$M_{k,k',\ell} = D_{N_F} \left( \frac{k' - k}{N_F} + \Delta F_\ell T \right) \quad (10)$$

$$\begin{aligned} D_M(x) &= \frac{1}{M} \sum_{m=0}^{M-1} e^{j2\pi m x} \\ &= e^{j\pi(M-1)x} \frac{\sin(\pi M x)}{M \sin(\pi x)} \end{aligned} \quad (11)$$

and  $W_{i,n,k}$  is the noise contribution, with  $E[W_{i,n,k} W_{i,n',k'}^*] = N_0 \delta_{n-n'}$ . The sequence  $\{\tilde{c}_{i,n,\ell}\}$  results from applying a rotation of  $2\pi \Delta F_\ell T (N_F + N_P)$  rad/chip to the chip sequence  $\{c_{i,n,\ell}\}$ . When  $M_{k,k',\ell}$  is nonzero for some  $k' \neq k$ , the  $k$ th FFT output gets interference from the symbol  $a_{i,k',\ell}$  that has been transmitted by user  $\ell$  on the carrier with index  $k'$ . When  $\Delta F_\ell = 0$ , the contribution from user  $\ell$  to the  $k$ th FFT output only contains the symbol  $a_{i,k,\ell}$  transmitted on the  $k$ th carrier.

The detection of the symbol  $a_{i,k,0}$  is based upon the decision variable  $z_{i,k}$ , which is given by

$$\begin{aligned} z_{i,k} &= \frac{1}{\sqrt{N_s}} \sum_{n=0}^{N_s-1} V_{i,n,k} g_{i,n,k} c_{i,n,0}^* \\ &= \sqrt{\frac{N_F}{N_F + N_P}} \sum_{\ell=0}^{N_u-1} \sum_{k' \in I_c} a_{i,k',\ell} I_{i,k,k',\ell} + W_{i,k} \end{aligned} \quad k \in I_c \quad (12)$$

where

$$I_{i,k,k',\ell} = \frac{H_{k',\ell} M_{k,k',\ell}}{N_s} \sum_{n=0}^{N_s-1} g_{i,n,k} c_{i,n,0}^* \tilde{c}_{i,n,\ell} \quad (13)$$

The quantity  $I_{i,k,k',\ell}$  denotes the contribution from the data symbol  $a_{i,k',\ell}$  to the sample  $z_{i,k}$  at the input of the decision device. The sample  $z_{i,k}$  from (12) contains a useful component with coefficient  $I_{i,k,k,0}$ . The quantities  $I_{i,k,k',0}$  ( $k' \neq k$ ) correspond to intercarrier interference (ICI), i.e., the contribution from data symbols transmitted by the reference user on other carriers. For  $\ell \neq 0$ , the quantities  $I_{i,k,k',\ell}$  correspond to multiuser interference (MUI), i.e., the contribution from data symbols transmitted by other users. The AWGN contribution is denoted  $W_{i,k}$ .

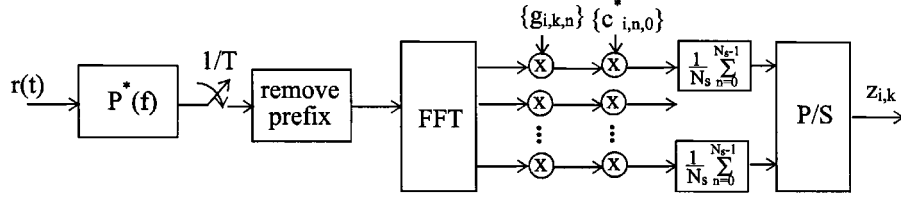


Fig. 4. MC-DS-CDMA receiver structure.

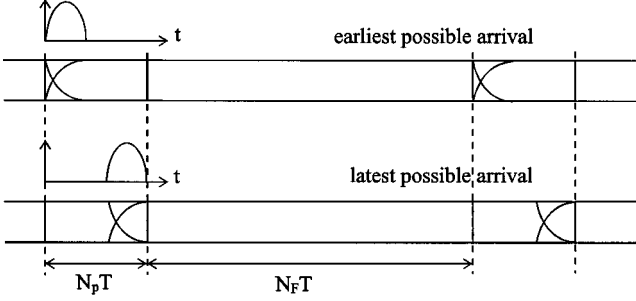


Fig. 5. Minimum cyclic prefix length to avoid interference between FFT blocks.

The equalizer coefficients are selected such that the coefficients  $I_{i,k,k,0}$  of the useful component equal one, for  $k \in I_c$ . This yields

$$g_{i,k,n} = \frac{e^{-j\phi_0(0)} e^{-j2\pi\Delta F_0 T(n+iN_s)(N_F+N_P)}}{H_{k,0} M_{k,k,0}}. \quad (14)$$

From (7), (9), (10), and (14), it follows that the one-tap equalizer compensates the scaling and the rotation of  $a_{i,k,0} c_{i,n,0}$  at the  $k$ th FFT output [assuming that accurate estimates of  $\phi_0(0)$ ,  $\Delta F_0 T$ , and  $H_{k,0}$  are available]. Substituting (14) into (13) yields

$$I_{i,k,k',\ell} = \frac{H_{k',\ell} M_{k,k',\ell}}{H_{k,0} M_{k,k,0}} \tilde{R}_{i,\ell} \quad (15)$$

where

$$\begin{aligned} \tilde{R}_{i,\ell} &= \frac{1}{N_s} \sum_{n=0}^{N_s-1} \tilde{c}_{i,n,0}^* \tilde{c}_{i,n,\ell} \\ &= \frac{e^{j(\phi_\ell(0)-\phi_0(0))}}{N_s} \sum_{n=0}^{N_s-1} c_{i,n,0}^* c_{i,n,\ell} \\ &\quad \cdot e^{j2\pi(\Delta F_\ell T - \Delta F_0 T)(n+iN_s)(N_F+N_P)} \end{aligned} \quad (16)$$

is the correlation between the sequences  $\{\tilde{c}_{i,n,\ell}\}$  and  $\{\tilde{c}_{i,n,0}\}$ . Noting that  $\tilde{R}_{i,0} = 1$ , it follows from (15) with  $\ell = 0$  that  $M_{k,k',0}$  with  $k' \neq k$  affects the components of the ICI. The components of the MUI are affected by  $\tilde{R}_{i,\ell}$  with  $\ell \neq 0$ . In general, the one-tap equalizer cannot eliminate the MUI and the ICI, i.e.,  $I_{i,k,k',0} \neq 0$  for  $k' \neq k$  and  $I_{i,k,k',\ell} \neq 0$  for  $\ell \neq 0$ .

It is instructive to consider the case where all frequency offsets are zero, i.e.,  $\Delta F_\ell = 0$  for  $\ell = 0, \dots, N_u - 1$ . In this case, we observe from (6) that the contribution of user  $\ell$  to the matched filter output samples  $\nu_{i,n,m}$  is proportional to the IFFT of  $b_{i,k',n,\ell} H_{k',\ell}$ . Hence, the contribution of user  $\ell$  to the  $k$ th

FFT output  $V_{i,n,k}$  is proportional to  $b_{i,k,n,\ell} H_{k,\ell}$ , which means that ICI is absent. In addition, as the factor  $H_{k,\ell}$  does not depend on the chip index, the orthogonality between the contributions from different users to the same FFT output is not affected (i.e.,  $\tilde{R}_{i,\ell} = 0$  for  $\ell \neq 0$ ); hence MUI is absent as well. This indicates that in the absence of carrier frequency offsets, the only effect of the multipath channel on the uplink MC-DS-CDMA signal with cyclic prefix is to multiply the symbols from each user with a factor  $H_{k,\ell}$  that depends on the user index and on the carrier index. The presence of this factor affects the signal-to-noise ratio (SNR) at the input of the decision device but does not give rise to interference.

### B. Downlink MC-DS-CDMA

In downlink MC-DS-CDMA, the basestation broadcasts to all users the sum of the  $N_u$  user signals  $s_\ell(t)$  from (3). As shown in Fig. 3(b), this broadcast signal reaches the receiver of the reference user through a multipath channel with transfer function  $H_{ch}(f)$ . The output of the channel is affected by a small carrier frequency offset  $\Delta F$ :  $\phi(t) = 2\pi\Delta F t + \phi(0)$  with  $|\Delta F T| \ll 1$ . The contributions from all users are affected by the same frequency offset because all user signals are upconverted by the same carrier oscillator at the basestation. Further, the received signal is disturbed by an AWGN process  $w(t)$ , whose real and imaginary parts are uncorrelated and have the same power spectral density  $N_0/2$ .

Similarly as in uplink MC-DS-CDMA, the received signal is applied to the receiver from Fig. 4 in order to detect the data symbols transmitted to the reference user ( $\ell = 0$ ). Assuming that the duration of the impulse response of the composite channel [with transfer function  $H(f) = |P(f)|^2 H_{ch}(f)$ ] does not exceed the cyclic prefix length, the sample  $z_{i,k}$  at the input of the decision device can be represented as in (12). The quantities  $I_{i,k,k',\ell}$  are given by (13), with  $H_{k,\ell}$ ,  $\phi_\ell(0)$ , and  $\Delta F_\ell T$  substituted by  $H_k = H(\text{mod}(k; N_F)/(N_F T))/T$ ,  $\phi(0)$ , and  $\Delta F T$ , respectively. As in the uplink, the samples  $z_{i,k}$  are decomposed into a useful component, ICI, MUI, and noise. The equalizer coefficients, selected such that the coefficients  $I_{i,k,k,0}$  of the useful component equal one, are given by (14), with  $H_{k,0}$ ,  $\phi_0(0)$ , and  $\Delta F_0 T$  substituted by  $H_k$ ,  $\phi(0)$ , and  $\Delta F T$ . The resulting equalizer not only compensates for the scaling and rotation of the useful component but also eliminates the MUI (i.e.,  $I_{i,k,k',\ell} = 0$  for  $\ell \neq 0$ ). However, this equalizer cannot eliminate the ICI.

The carrier frequency offset does not yield MUI in downlink MC-DS-CDMA because all users are affected by the *same* offset  $\Delta F$ . This implies that the equalizer, which compensates the rotation of  $2\pi\Delta F T$  rad/sample of the reference user signal, automatically compensates the rotation of the other user signals as

well, hence maintaining orthogonality of the different user signals. Stated mathematically, in downlink transmission the quantity  $\tilde{R}_{i,\ell}$  equals the correlation of the original chip sequences  $\{c_{i,n,\ell}\}$  and  $\{c_{i,n,0}\}$ , so that orthogonal spreading sequences yield  $\tilde{R}_{i,k,k',\ell} = 0$  for  $\ell \neq 0$  [see (13)]. This indicates that, even in the presence of a carrier frequency offset, the multipath distortion affecting the downlink MC-DS-CDMA signal with cyclic prefix does not give rise to multiuser interference.

### III. PERFORMANCE ANALYSIS

#### A. Uplink MC-DS-CDMA

The performance of the MC-DS-CDMA system is measured by the SNR, which is defined as the ratio of the power of the useful component ( $P_U$ ) to the sum of the powers of the intercarrier interference ( $P_{ICI}$ ), the multiuser interference ( $P_{MUI}$ ), and the noise ( $P_N$ ) at the input of the decision device. Note that these quantities depend on the index  $k$  of the considered carrier. This yields

$$\text{SNR}_k(\Delta \mathbf{F}T) = \frac{\frac{N_F}{N_F + N_P} P_{U_k}}{P_{N_k} + \frac{N_F}{N_F + N_P} (P_{ICI_k} + P_{MUI_k})} \quad (17)$$

where  $\Delta \mathbf{F} = (\Delta F_0, \Delta F_1, \dots, \Delta F_{N_u-1})$ . In (17), the powers of the useful component, ICI, MUI, and noise are given by

$$\begin{aligned} P_{U_k} &= E_{s_{k,0}} \\ P_{ICI_k} &= \sum_{\substack{k' \in I_c \\ k' \neq k}} E_{s_{k',0}} \left| \frac{H_{k',0}}{H_{k,0}} \right|^2 \frac{X_{k,k',0}}{X_{0,0,0}} \\ P_{MUI_k} &= \frac{1}{N_s - 1} \sum_{\ell=1}^{N_u-1} \left( \sum_{k' \in I_c} E_{s_{k',\ell}} \left| \frac{H_{k',\ell}}{H_{k,0}} \right|^2 \frac{X_{k,k',\ell}}{X_{0,0,0}} \right) Y_\ell \\ P_{N_k} &= \frac{N_0}{|H_{k,0}|^2 X_{0,0,0}} \end{aligned} \quad (18)$$

with

$$\begin{aligned} X_{k,k',\ell} &= \left| D_{N_F} \left( \frac{k' - k}{N_F} + \Delta F_\ell T \right) \right|^2 \\ Y_\ell &= \left( 1 - |D_{N_s}((N_F + N_P)(\Delta F_\ell - \Delta F_0)T)|^2 \right). \end{aligned} \quad (19)$$

In (18),  $E_{s_{k,\ell}} = E[|a_{i,k,\ell}|^2]$  denotes the symbol energy transmitted on carrier  $k$  by user  $\ell$ . The MUI power from (18) represents an average over all possible assignments of the orthogonal spreading sequences to the users. In the absence of carrier frequency offsets ( $\Delta \mathbf{F} = 0$ ), the SNR (17) reduces to  $\text{SNR}_k(0) = (N_F/(N_F + N_P))|H_{k,0}|^2(E_{s_{k,0}}/N_0)$ . The degradation (in dB), caused by the carrier frequency offset, is defined as  $\text{Deg}_k = 10 \log(\text{SNR}_k(0)/\text{SNR}_k(\Delta \mathbf{F}T))$ .

To clearly isolate the effect of the carrier frequency offsets, we assume that the channels are ideal and all users have the same energy per symbol on each carrier (i.e.,  $|H_{k,\ell}| = 1$  and

$E_{s_{k,\ell}} = E_s$  for  $k \in I_c, \ell = 0, \dots, N_u - 1$ ). In this case, the degradation is given by

$$\begin{aligned} \text{Deg}_k &= -10 \log(X_{0,0,0}) \\ &+ 10 \log \left( 1 + \text{SNR}(0) \left( \sum_{\substack{k' \in I_c \\ k' \neq k}} X_{k,k',0} + \frac{1}{N_s - 1} \right. \right. \\ &\quad \left. \left. \cdot \sum_{\ell=1}^{N_u-1} \left( \sum_{k' \in I_c} X_{k,k',\ell} \right) Y_\ell \right) \right) \end{aligned} \quad (20)$$

where  $\text{SNR}(0) = (N_F/(N_F + N_P))(E_s/N_0)$ . The summation over  $k'$  in (20) ranges over the set  $I_c$  of  $N_c$  modulated carriers. A simple upper bound on the degradation is obtained by extending in (20) this summation over all  $N_F$  available carriers, i.e.,  $k' = 0, \dots, N_F - 1$ . This yields

$$\begin{aligned} \text{Deg} &\leq -10 \log(X_{0,0,0}) \\ &+ 10 \log \left( 1 + \text{SNR}(0) \right. \\ &\quad \left. \cdot \left( 1 - X_{0,0,0} + \frac{1}{N_s - 1} \sum_{\ell=1}^{N_u-1} Y_\ell \right) \right) \end{aligned} \quad (21)$$

which is independent of the carrier index  $k$ . This upper bound is reached when all carriers are modulated ( $N_c = N_F; \alpha = 0$ ). When  $\alpha > 0$ , the upper bound (21) yields an accurate approximation for the actual degradation on carriers near the center of the signal band.

#### B. Downlink MC-DS-CDMA

As in uplink MC-DS-CDMA, the performance is measured by the SNR defined in (17). The powers of the useful component, the intercarrier interference, the multiuser interference, and the noise are given by (18), with  $H_{k,\ell}$  and  $\Delta F_\ell T$  substituted by  $H_k$  and  $\Delta F T$ , respectively, for  $\ell = 0, 1, \dots, N_u - 1$ . In this case, it follows from (11) and (19) that  $Y_\ell = 0$ . This expresses that, in contrast with uplink MC-DS-CDMA, MUI is absent in downlink transmission [see (18)]. The degradation of the SNR is defined in a similar way as in the uplink (with  $H_{k,0} = H_k$  and  $\Delta F_0 = \Delta F$ ). For given  $N_F$  and  $\Delta F T$ , this degradation is independent of the spreading factor  $N_s$  and of the characteristics of the other users.

To clearly isolate the effect of the carrier frequency offset, we consider the case where the channel is ideal ( $|H_k| = 1, k \in I_c$ ), and the energy per symbol is the same for all carriers and all users ( $E_{s_{k,\ell}} = E_s$  for  $k \in I_c, \ell = 0, \dots, N_u - 1$ ). The resulting degradation is given by

$$\begin{aligned} \text{Deg}_k &= -10 \log(X_{0,0,0}) \\ &+ 10 \log \left( 1 + \text{SNR}(0) \left( \sum_{k' \in I_c} X_{k,k'} - X_{0,0,0} \right) \right) \end{aligned} \quad (22)$$

with

$$X_{k,k'} = \left| D_{N_F} \left( \frac{k' - k}{N_F} + \Delta FT \right) \right|^2. \quad (23)$$

As in uplink transmission, an upper bound on the degradation is obtained by extending the summation over  $k'$  in (22) over all  $N_F$  available carriers, yielding

$$\text{Deg} \leq -10 \log(X_{0,0}) + 10 \log(1 + \text{SNR}(0)(1 - X_{0,0})) \quad (24)$$

which is independent of the carrier index  $k$ . The upper bound (24) is only a function of  $\text{SNR}(0)$  and  $X_{0,0}$ . This upper bound is reached when all carriers are modulated ( $N_c = N_F$ ;  $\alpha = 0$ ). For  $\alpha > 0$ , the upper bound yields an accurate approximation for the actual degradation on carriers near the center of the signal band.

#### IV. COMPARISON OF DEGRADATIONS IN UPLINK AND DOWNLINK MC-DS-CDMA

When the frequency offset  $\Delta F$  in downlink transmission is the same as the frequency offset  $\Delta F_0$  for the reference user in uplink transmission, it follows from (18) that the powers of the useful signal, the ICI, and the noise in downlink transmission are the same as in uplink transmission. Hence, the degradation in the uplink is larger than in the downlink, because MUI is absent in the latter.

Let us assume that all carrier frequency offsets are within the interval  $[-F_{\max}, F_{\max}]$ , where  $F_{\max}$  is restricted to be smaller than the carrier spacing, i.e.,  $F_{\max} < \Delta f = 1/(N_F T)$ . For small  $x$ , the approximation  $\sin(\pi x) \cong \pi x$  holds, such that  $|D_M(x)| \cong \sin(\pi Mx)/(\pi Mx)$  [see (11)]. Hence, when  $N_F \gg 1$ ,  $X_{0,0,0}$  from (19) and  $X_{0,0}$  from (23) are essentially functions of  $N_F \Delta F_0 T$  and  $N_F \Delta FT$ , respectively. In uplink transmission, we consider the case where  $N_u \gg 1$  and the frequency offsets  $\Delta F_\ell$  for  $\ell > 0$  are uniformly distributed in the interval  $[-F_{\max}, F_{\max}]$ ; in this case, (21) reduces to

$$\begin{aligned} \text{Deg} \leq & -10 \log(X_{0,0,0}) \\ & + 10 \log \left( 1 + \text{SNR}(0) \left( 1 - X_{0,0,0} + \frac{N_u - 1}{N_s - 1} \bar{Y} \right) \right) \end{aligned} \quad (25)$$

where

$$\begin{aligned} \bar{Y} = & 1 - \frac{1}{2F_{\max}T} \int_{-F_{\max}T}^{F_{\max}T} \\ & \cdot \left( \frac{\sin(\pi N_s(N_F + N_P)(x - \Delta F_0 T))}{N_s \sin(\pi(N_F + N_P)(x - \Delta F_0 T))} \right)^2 dx. \end{aligned} \quad (26)$$

Note that  $\bar{Y}$  still depends on  $\Delta F_0$ . In the following, we look for the values of  $\Delta F$  and  $\Delta F_0$  that maximize (24) and (25), respectively, and we compare the corresponding maximum degradations.

The bound (24) on downlink degradation is a decreasing function of  $X_{0,0}$ . Taking into account (23), the condition  $|\Delta FT| < 1/N_F$ , and the behavior of the function  $|D_M(x)|$  (see Fig. 6), it follows that the maximum value of (the bound on) the degradation (24) occurs when  $|\Delta F|$  assumes its maximum value, i.e.,

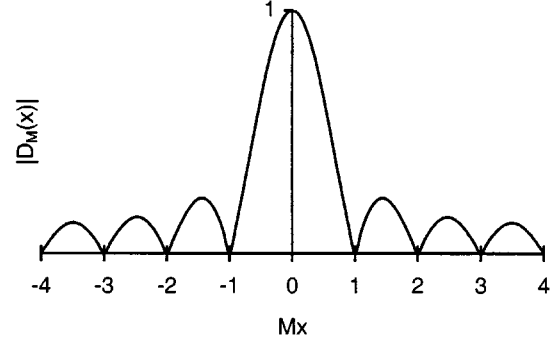


Fig. 6. Shape of  $|D_M(x)|$ ,  $M = 8$ .

$|\Delta F| = F_{\max}$ . This maximum degradation is given by (24), with

$$X_{0,0} = \left| \frac{\sin(\pi N_F F_{\max} T)}{N_F \sin(\pi F_{\max} T)} \right|^2. \quad (27)$$

For given  $N_F \Delta FT$ , the maximum degradation does not depend on the spreading factor.

The bound (25) on uplink degradation is decreasing with  $X_{0,0,0}$  but increasing with  $\bar{Y}$ . A similar reasoning as for downlink transmission shows that  $X_{0,0,0}$  is minimum for  $|\Delta F_0| = F_{\max}$ . Moreover, it turns out that  $\bar{Y}$  is maximum for  $|\Delta F_0| = F_{\max}$ . Hence, the maximum uplink degradation is given by (25), with

$$\begin{aligned} X_{0,0,0} = & \left| \frac{\sin(\pi N_F F_{\max} T)}{N_F \sin(\pi F_{\max} T)} \right|^2 \\ \bar{Y} = & 1 - \frac{1}{2F_{\max}T(N_F + N_P)} \int_0^{2F_{\max}T(N_F + N_P)} \\ & \cdot \left( \frac{\sin(\pi N_s x)}{N_s \sin(\pi x)} \right)^2 dx \\ \cong & 1 - \frac{1}{2F_{\max}N_F T} \int_0^{2F_{\max}N_F T} \\ & \cdot \left( \frac{\sin(\pi N_s x)}{N_s \sin(\pi x)} \right)^2 dx \end{aligned} \quad (28)$$

where the approximation in (29) holds for  $N_F \gg N_P$ .

Assuming  $N_u = N_s$  (maximum load), the maximum uplink and downlink degradations at  $\text{SNR}(0) = 10$  dB are shown in Fig. 7 as a function of  $F_{\max}/\Delta f = N_F F_{\max} T = N_c(F_{\max}/B) = (N_c/N_s)(F_{\max}/R_s)$  for several values of the spreading factor  $N_s$ .

- 1) For given  $\text{SNR}(0)$ , the downlink degradation depends only on the ratio  $F_{\max}/\Delta f$ . Hence, for given  $F_{\max}/B$ , this degradation increases with the number ( $N_c$ ) of carriers. Stated otherwise, for given  $F_{\max}/R_s$ , the degradation increases with the ratio  $N_c/N_s$ . To obtain small degradations, the carrier frequency offset must be kept small as compared to the carrier spacing of the multicarrier system, i.e.,  $F_{\max} \ll \Delta f$ . In this case, the degradation is essentially proportional to  $(F_{\max}/\Delta f)^2 = (N_F F_{\max} T)^2 = (N_c F_{\max}/B)^2 = ((N_c/N_s)(F_{\max}/R_s))^2$ .

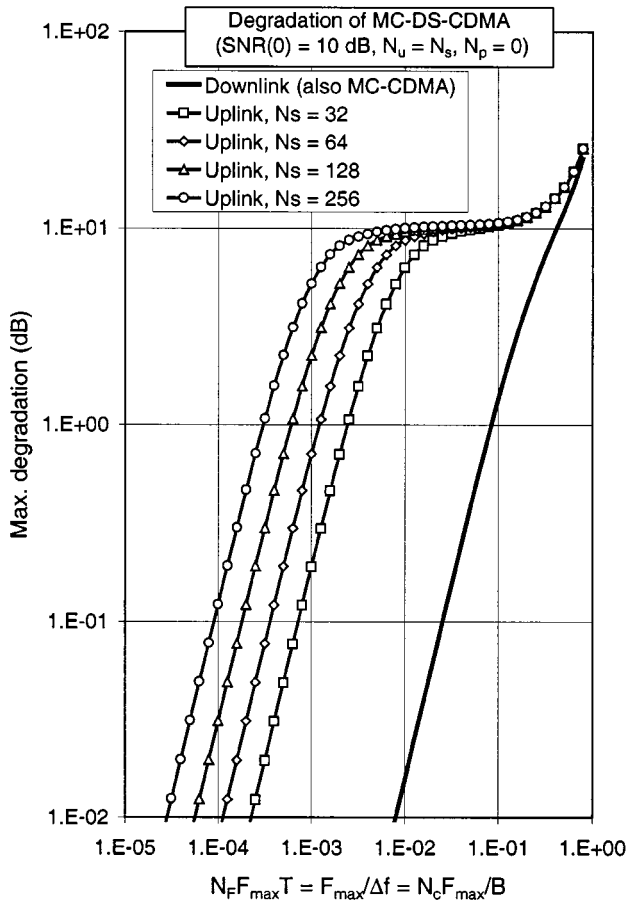


Fig. 7. Maximum degradation caused by carrier frequency offset.

- 2) We observe that the maximum degradation is much larger in the uplink than in the downlink. This indicates that the uplink degradation is dominated by the MUI. For  $F_{\max} \gg \Delta f / (2N_s)$ , we have  $\bar{Y} \cong 1$  [see (29)], in which case the maximum uplink degradation (25) depends only on the ratio  $F_{\max} / \Delta f$ . In this region, the curves in Fig. 7 coincide for different values of  $N_s$ ; for given  $F_{\max} / B$  or  $F_{\max} / R_s$ , the corresponding degradation increases with  $N_c$  or  $N_c / N_s$ , respectively. A small degradation can be obtained only when  $F_{\max} \ll \Delta f / (2N_s)$ . As compared to the downlink, this condition on  $F_{\max}$  is more stringent by a factor of  $2N_s$ . For  $F_{\max} \ll \Delta f / (2N_s)$ , the degradation is essentially proportional to  $(N_s F_{\max} / \Delta f)^2 = (N_s N_F F_{\max} T)^2 = (N_s N_c F_{\max} / B)^2 = (N_c F_{\max} / R_s)^2$ ; in this region, the ratio between uplink and downlink degradation is proportional to  $N_s^2$ .

## V. COMPARISON WITH MC-CDMA

In the case of MC-CDMA, the original data stream at rate  $R_s$  is first multiplied with the spreading sequence and then modulated on the orthogonal carriers. This is accomplished by means of an  $N_F$ -point IFFT, which is cyclically extended with a prefix of  $N_P$  samples. In contrast with MC-DS-CDMA, where the spreading is done in the time domain, in MC-CDMA the  $N_s$  chips belonging to the same symbol are modulated on different

carriers: the spreading is done in the frequency domain (see Fig. 8). Here we consider the basic MC-CDMA scheme, where the number of modulated carriers is the same as the spreading factor  $N_s$ . The corresponding sampling rate is  $1/T = (N_F + N_P)R_s$ , and the resulting carrier spacing  $\Delta f$  and the system bandwidth  $B$  are given by

$$\Delta f = \frac{1}{N_F T} = R_s \frac{N_F + N_P}{N_F} \cong R_s$$

$$B = N_s \Delta f = \frac{N_s}{N_F T} = N_s R_s \frac{N_F + N_P}{N_F} \cong N_s R_s. \quad (30)$$

Comparing (30) and (4), we observe that for a given symbol rate  $R_s$  and given spreading factor  $N_s$ , MC-DS-CDMA and MC-CDMA yield essentially the same system bandwidth. However, the carrier spacing in MC-DS-CDMA is  $N_s / N_c$  times the carrier spacing in MC-CDMA.

The considered receiver for MC-CDMA is similar to the MC-DS-CDMA receiver from Fig. 4. The receiver takes the FFT of  $N_F$  matched filter output samples located outside the cyclic prefix. Each FFT output is followed by a one-tap equalizer that compensates for the effect of the carrier frequency offset and the multipath channel [10]. The equalizer outputs are multiplied with the complex conjugate of the chip of the reference user on the corresponding carrier and summed over the  $N_s$  carriers to form the decision variable on which the detection of the data symbol is based.

It has been shown in [10] that, in the absence of frequency offset, the decision variable corresponding to downlink transmission is not affected by interference because the user signals transmitted by the basestation are synchronized in time and affected by the same multipath channel. In uplink MC-CDMA, the different user signals are not aligned in time and are sent over different multipath channels; this gives rise to significant MUI that cannot be compensated by the one-tap equalizers, even in the absence of frequency offsets. To combat MUI in uplink MC-CDMA, a much more complicated receiver structure is required. As such receivers are beyond the scope of this paper, we restrict our attention to downlink MC-CDMA with the "simple" receiver performing one-tap equalization on each carrier. Note that in uplink MC-DS-CDMA, the problems encountered in uplink MC-CDMA do not occur, as the spreading in MC-DS-CDMA is done in the time domain.

In [10], the effect of a carrier frequency offset on downlink MC-CDMA has been investigated. Similarly as in MC-DS-CDMA, a tight upper bound on the degradation has been derived:

$$\text{Deg} \leq -10 \log(X_{0,0}) + 10 \log \left( 1 + \text{SNR}(0) \frac{N_u}{N_s} (1 - X_{0,0}) \right) \quad (31)$$

where  $X_{0,0}$  is given by (23) and  $N_u$  denotes the number of users. The upper bound is reached when all  $N_F$  carriers are modulated. For  $|\Delta FT| \ll 1$ , the upper bound is only a function of  $\text{SNR}(0)$ , the load  $N_u / N_s$ , and  $N_F \Delta FT = \Delta F / \Delta f$ .

The degradation (24) for MC-DS-CDMA is caused by ICI from the reference user, and therefore does not depend on the load, whereas the degradation (31) for MC-CDMA is caused

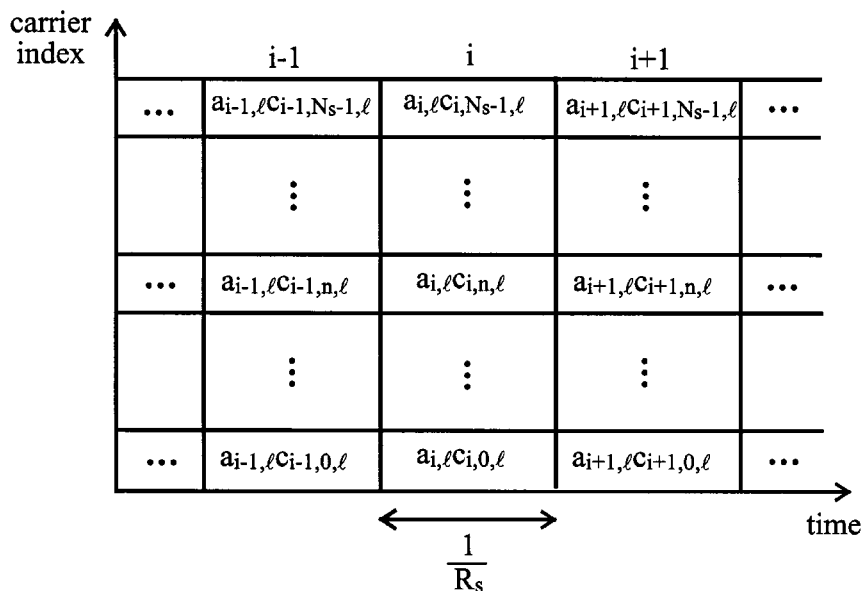


Fig. 8. Illustration of frequency-domain spreading in MC-CDMA.

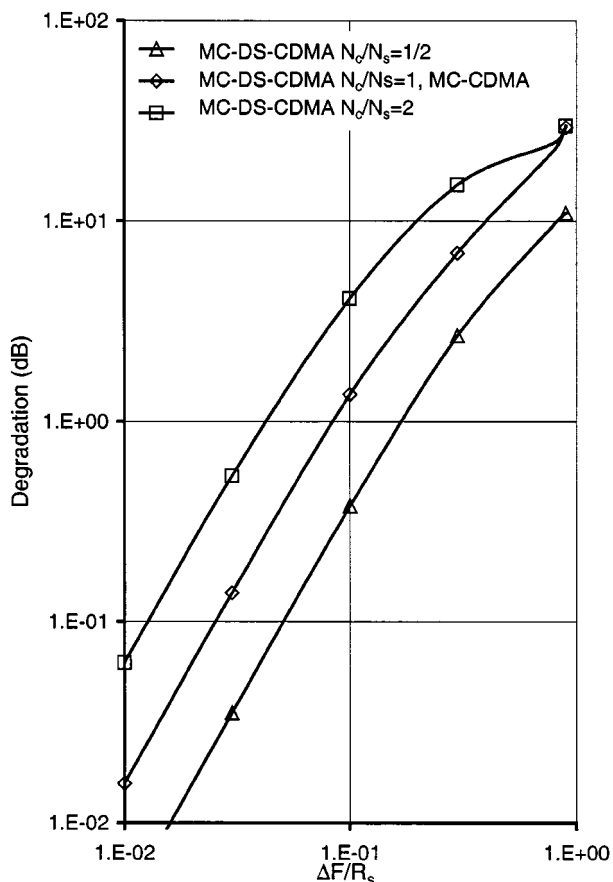


Fig. 9. Downlink degradation for MC-DS-CDMA and MC-CDMA.  $N_u = N_s$  and  $SNR(0) = 10$  dB.

by MUI, and therefore increases with the load. For given  $N_F \Delta FT = \Delta F / \Delta f$ , the degradations of MC-DS-CDMA and MC-CDMA are the same at maximum load ( $N_u = N_s$ ).

Now let us compare (24) and (31) at maximum load, for a given  $R_s$  and  $N_s$ . It follows from (4) and (30) that the carrier spacing for MC-DS-CDMA is larger (smaller) than for

MC-CDMA when  $N_s$  is larger (smaller) than  $N_c$ . Hence, for a given frequency offset  $\Delta F$ , MC-DS-CDMA yields the smaller (larger) degradation when  $N_s$  is larger (smaller) than  $N_c$ . This is illustrated in Fig. 9, where the bounds (24) and (31) are shown as a function of  $\Delta F / R_s$  for the maximum load and for various values of  $N_c / N_s$ .

### VI. CONCLUSION

In this paper, we have investigated the effect of carrier frequency offsets on uplink and downlink performance of MC-DS-CDMA with orthogonal spreading sequences. Our conclusions can be summarized as follows.

- 1) In the uplink, carrier frequency offsets give rise to a reduction of the useful signal power and to the occurrence of ICI and MUI. In the downlink, MUI is absent. Hence, frequency offsets cause a larger degradation in the uplink than in the downlink.
- 2) In both the uplink and the downlink, the degradation strongly increases with the ratio  $F_{\max} / \Delta f$  of maximum frequency offset to carrier spacing.
- 3) For given  $F_{\max} / \Delta f$ , the degradation in the downlink does not depend on the spreading factor  $N_s$ . Achieving a small degradation requires  $F_{\max} / \Delta f \ll 1$ , in which case the degradation is proportional to  $(F_{\max} / \Delta f)^2$ .
- 4) For given  $F_{\max} / \Delta f$  and assuming a fully loaded system ( $N_u = N_s$ ), the degradation in the uplink increases with the spreading factor  $N_s$ . Achieving a small degradation requires  $F_{\max} / \Delta f \ll 1 / (2N_s)$ , a condition that is much more stringent than in the downlink, especially when the spreading factor is large. The corresponding degradation is larger than in the downlink by a factor that is proportional to  $N_s^2$ .

Finally, we have compared the sensitivities of MC-CDMA and MC-DS-CDMA to carrier frequency offset in the downlink. MC-CDMA is affected by MUI, and therefore the degradation increases with the load. For a given spreading factor and symbol



rate, the MC-CDMA system at maximum load is less (more) sensitive to carrier frequency offset than MC-DS-CDMA when the number of modulated carriers in MC-DS-CDMA is smaller (larger) than in MC-CDMA.

#### REFERENCES

- [1] R. van Nee and R. Prasad, *OFDM for Wireless Multimedia Communications*. Reading, MA: Artech House, 2000.
- [2] Z. Wang and G. B. Giannakis, "Wireless multicarrier communications," *IEEE Signal Processing Mag.*, vol. 17, pp. 29–48, May 2000.
- [3] N. Morinaga, M. Nakagawa, and R. Kohno, "New concepts and technologies for achieving highly reliable and high capacity multimedia wireless communication systems," *IEEE Commun. Mag.*, vol. 38, pp. 34–40, Jan. 1997.
- [4] G. Santella, "Bit error rate performances of M-QAM orthogonal multicarrier modulation in presence of time-selective multipath fading," in *Proc. ICC'95*, Seattle, WA, June 1995, pp. 1683–1688.
- [5] S. Kondo and L. B. Milstein, "Performance of multicarrier DS-SS systems," *IEEE Trans. Commun.*, vol. 44, pp. 238–246, Feb. 1996.
- [6] S. Hara and R. Prasad, "Overview of multicarrier CDMA," *IEEE Commun. Mag.*, vol. 35, no. 12, pp. 126–133, 1997.
- [7] V. M. DaSilva and E. S. Sousa, "Performance of orthogonal CDMA sequences for quasisynchronous communication systems," in *Proc. IEEE ICUPC'93*, Ottawa, ON, Canada, Oct. 1993, pp. 995–999.
- [8] E. A. Sourour and M. Nakagawa, "Performance of orthogonal multicarrier CDMA in a multipath fading channel," *IEEE Trans. Commun.*, vol. 44, pp. 356–367, Mar. 1996.
- [9] T. Pollet, M. Van Bladel, and M. Moeneclaey, "BER sensitivity of OFDM systems to carrier frequency offset and Wiener phase noise," *IEEE Trans. Commun.*, vol. 43, pp. 191–193, Feb./Mar./Apr. 1993.
- [10] H. Steendam and M. Moeneclaey, "The effect of synchronization errors on MC-CDMA performance," in *Proc. ICC'99*, Vancouver, BC, Canada, June 1999, Paper S38.3, pp. 1510–1514.
- [11] L. Tomba and W. A. Krzymien, "Effect of carrier phase noise and frequency offset on the performance of multicarrier CDMA systems," in *Proc. ICC'96*, Dallas, TX, June 1996, Paper S49.5, pp. 1513–1517.

**Heidi Steendam** received the diploma and the Ph.D. degree in electrical engineering from the University of Gent, Gent, Belgium, in 1995 and 2000, respectively.

She is with the Department of Telecommunications and Information Processing, University of Gent, as a Postdoctoral Researcher. Her main research interests are in statistical communication theory, carrier and symbol synchronization, bandwidth-efficient modulation and coding, spread-spectrum (multicarrier spread-spectrum), and satellite and mobile communication.



**Marc Moeneclaey** (M'93–SM'99) received the diploma of electrical engineering and the Ph.D. degree in electrical engineering from Ghent University, Ghent, Belgium, in 1978 and 1983, respectively.

In the period from 1978 to 1999, he held at Ghent University various positions for the Belgian National Fund for Scientific Research (NFWO), from Research Assistant to Research Director. He is presently a Professor in the Department of Telecommunications and Information Processing (TELIN), Ghent University. His research interests

include statistical communication theory, carrier and symbol synchronization, bandwidth-efficient modulation and coding, spread-spectrum, satellite and mobile communication. He is the author of more than 200 scientific papers in international journals and conference proceedings. Together with H. Meyr (RWTH Aachen) and S. Fechtel (Siemens AG), he co-authored the book *Digital Communication Receivers—Synchronization, Channel Estimation, and Signal Processing* (New York: Wiley, 1998).

From 1992 to 1994, he served as Editor for Synchronization, for the IEEE TRANSACTIONS ON COMMUNICATIONS. Since 1993, he has been an Executive Committee Member of the IEEE Communications and Vehicular Technology Society Joint Chapter, Benelux Section. He has been active in various international conferences as Technical Program Committee member and Session chairman.